Applied Clay Science 51 (2011) 267–273

Contents lists available at ScienceDirect

Applied Clay Science

journal homepage: www.elsevier.com/locate/clay

Comparative study between catalysts for esterification prepared from kaolins

Luís Adriano S. do Nascimento [a,*], Rômulo S. Angélica [b], Carlos E.F. da Costa [a], José R. Zamian [a], Geraldo N. da Rocha Filho [a]

[a] Laboratório de Catálise e Oleoquímica, Universidade Federal do Pará, Rua Augusto Corrêa, Guamá, CEP: 66075-110, Belém, Pará, Brasil
[b] Laboratório de Difração de Raios-X, Universidade Federal do Pará, Rua Augusto Corrêa, Guamá, CEP: 66075-110, Belém, Pará, Brasil

ARTICLE INFO

Article history:
Received 21 July 2010
Received in revised form 19 November 2010
Accepted 24 November 2010
Available online 28 November 2010

Keywords:
Acid leaching
Metakaolin
Microporous
Esterification
Oleic acid

ABSTRACT

The esterification of free fatty acids (FFA) is an alternative for the production of biodiesel from oils with high concentrations of FFA. In this paper, catalysts for the esterification of oleic acid with methanol were prepared from two Amazon kaolins (Century and *flint*) and two standard kaolins (KGa-1b and KGa-2) that were thermally treated at 950 °C and leached with 4 M sulfuric acid solutions. The activated metakaolin samples were characterized by X-ray diffraction, scanning electron microscopy, N_2 adsorption–desorption and pyridine adsorption studies using TG/DTG and FTIR analysis. The leached metakaolin prepared from Century showed the lowest Al content, the highest number of acidic sites (250.5 μmolPy/g) and offered larger conversion values. The influences of reaction parameters, such as temperature and time, were also investigated. Based on the catalytic results, kaolin was found to be a promising raw material for the production of new solid acid catalysts for the esterification of FFA. In particular, Amazonian *flint* kaolin, previously considered unusable for biofuel, was found to be amenable to production.

1. Introduction

The production of sustainable alternative fuels is attracting increasing academic and industrial interest. Biodiesel, a non-petroleum-based, is one of these sustainable fuels and boasts many advantages such as low emissions, biodegradability and better lubricity (Jacobson et al., 2008). Biodiesel consists of alkyl esters derived from either the transesterification of triglycerides (TG) in oils and fats or the esterification of free fatty acids (FFA) with short-chained alcohols (Boz et al., 2009; Jacobson et al., 2008).

The production of biodiesel by transesterification has a drawback because the utilization of high FFA feeds in traditional biodiesel production processes leads to depletion of the catalysts, as well as increased purification costs, because the FFA is saponified by the homogeneous alkaline catalyst, producing excess soap (Zheng et al., 2006). Esterification of FFA to alkyl esters in the presence of an acidic catalyst is a route to improve the use of high FFA oils in biodiesel production (Carmo Jr. et al., 2009). Esterification is normally carried out in a homogeneous phase in the presence of acid catalysts such as H_2SO_4, HF, H_3PO_4, HCl and p-toluene sulfonic acid (Carmo Jr. et al., 2009; Srilatha et al., 2009). This pretreatment step has been successfully demonstrated using sulfuric acid (Marchetti and Errazu, 2008). Unfortunately, the use of the homogeneous sulfuric acid catalyst adds neutralization and separation steps, as well as the esterification reaction, to the synthetic process (Mbaraka et al., 2003). Moreover, these catalysts are dangerous to use because they are hazardous and corrosive liquid acids (Srilatha et al., 2009). Therefore, heterogeneous catalysts can be considered as an alternative to minimize environmental damage and reduce biodiesel cost.

There are several works that deal with the production of catalysts using sulfonated carbons (Liu et al., 2008; Mo et al., 2008), modified zirconias (López et al., 2008), mesoporous sulfonic acid (Mbaraka and Shanks, 2006), heteropoly acid-based catalysts (Xu et al., 2009) and MCM (Carmo Jr. et al., 2009). However, there are few studies on the use of clay-based catalysts in the esterification of fatty acids. One such study is a report by Kantam et al. (2002) where Fe^{3+}-montmorillonite was used for the esterification of stearic acid with methanol.

Clay catalysts are interesting materials not only because of the low cost of their raw materials (Vaccari, 1999), but also because they are less harmful to the environment (Rezende, 2006). In addition, acid-activation is one of the modifications that can be made in clays (Araújo Melo et al., 2000; Flessner et al., 2001). This causes the disaggregation of clay particles, elimination of impurities and dissolution of external layers, altering the chemical composition and the structure of clays (Belver et al., 2002). The main consequences of acid activation are increases in surface area, porosity and number of acidic sites compared to the parent clays (Lenarda et al., 2007). Acid-treated montmorillonites are offered from various companies as catalysts for hydrocarbon cracking, such as the well-known commercial montmorillonite clay K-10, whose surface acidity and catalytic activity can be enhanced considerably through exchange with transition metal ions (Centi and Perathoner, 2008). However, the

* Corresponding author. Tel./fax: +55 91 32336331.
E-mail address: adrlui1@yahoo.com.br (L.A.S. do Nascimento).

0169-1317
doi:10.1016/j.clay.2010.11.030

catalytic activity of another major group of clay minerals, kaolinite, remains poorly studied.

The Amazon region, specifically northeastern Pará state, possesses the largest Brazilian reserves of high-whiteness kaolin (Carneiro et al., 2003). This kaolin is inserted in the Ipixuna Formation, where it is possible to distinguish between two main kaolin units (Carneiro et al., 2003) (Fig. 1). The first one is the inferior unit, which is mainly formed of kaolin and whose base contains the *soft* kaolin that is used in paper coating; the second is the *flint* or *semi-flint* kaolin (Kotschoubey et al., 1996). The *flint* kaolin is not used in the kaolin industry because it is an iron-rich kaolin, and requires additional cost to be extracted and separated from *soft* kaolin (Carneiro et al., 2003). Specifically, Century kaolin is a product of Pará Pigmentos S/A and consists of a kaolin of high purity and whiteness resulting from the processing of *soft* kaolin.

Considering these facts, this paper reports the preparation, characterization and catalytic tests of acid-activated metakaolins prepared from Amazon *flint* and Century kaolins in the esterification of oleic acid with methanol. The same procedures were performed with KGa-1b and KGa-2 kaolinites (Georgia State, USA) from Clay Minerals Society Source Clay for comparative studies.

2. Experimental section

2.1. Materials

The chemicals used in this report were oleic acid (synthetic grade) and methanol (AR grade) purchased from Aldrich and Synth (Brazil). The *flint* kaolin used in this study was collected in a mine located in the Rio Capim area (Pará-Brazil). The *flint* kaolin was triturated, and the sandy fraction was separated by retention in a sieve. The fraction below 62 μm was then collected, diluted in distilled water, sonicated and centrifuged for separation of the silt fraction and collection of the clay fraction. The Century kaolin was kindly provided by Pará Pigmentos S/A; KGa-1b and KGa-2 kaolins were purchased from the Clay Minerals Society. The Century, KGa-1b and KGa-2 kaolins were used as received.

2.2. Methods

2.2.1. Thermal treatment and acid activation of the kaolins

Kaolin is resistant to acid leaching due to its high octahedral aluminum content. The transformation of kaolin into metakaolin would then make this material more susceptible to the leaching of aluminum and iron cations from the octahedral layer (Lenarda et al., 2007). The phase transformations that occur when kaolin is calcined at high temperatures are demonstrated by the chemical reactions illustrated below (Carneiro et al., 2003):

$$\underset{\text{Kaolinite}}{2\ SiO_2{\cdot}Al_2O_3{\cdot}2H_2O} \xrightarrow[\sim 537\ ^\circ C]{} \underset{\text{Metakaolinite}}{2\ SiO_2{\cdot}Al_2O_3} + 2H_2O(g)$$

$$\underset{\text{Metakaolinite}}{2\ SiO_2{\cdot}Al_2O_3} \xrightarrow[\sim 983^\circ C]{} \underset{\text{Primary 1:1 mullite (Al–Si spinel)}}{Al_2O_3{\cdot}SiO_2} + \underset{\text{(amorphous)}}{SiO_2}$$

Samples of *flint*, Century, KGa-1b and KGa-2 kaolinites were calcined at 950 °C, providing metakaolin samples that were labeled MF9, MC9, M19 and M29, respectively. The metakaolin samples were then activated at 90 °C for 1 h with 4 M sulfuric acid solutions and then washed with distilled water, dried at 120 °C for 12 h and calcined at 400 °C for an additional 2 h. The four leached metakaolin samples obtained were designated MF9S4, MC9S4, M19S4 and M29S4, respectively.

2.2.2. Characterization

The chemical composition analysis was performed using a Shimadzu EDX-700 energy dispersive X-ray (EDX) spectrometer.

X-ray diffractions were obtained using a PANalytical X´PERT PRO MPD (PW 3040/60) diffractometer, using the powder method, at °5<2θ>70° intervals. CuKα and CoKα (40 kV and 40 mA) radiations were used. The 2θ scanning speed was 0.02°/s.

N_2 adsorption–desorption isotherms were obtained at liquid nitrogen temperature using a Quantachrome Nova 1200 apparatus. Before each measurement, the samples were outgassed at 130 °C for 2 h. The specific surface area, the microporous area, the microporous volume and the pore-size distribution were obtained, respectively, using Brunauer–Emmett–Teller (BET) and t-plot methods.

The morphology of the samples was inspected using a ZEISS microscope, model LEO 1430, operating at 10 kV and 90 mA. The samples were supported on carbon tapes and metalized with gold under vacuum conditions.

Thermogravimetry (TG) and derivative thermogravimetry (DTG) have been extensively used in catalyst characterization because they allow for the rapid evaluation of material changes in response to temperature variations (Ghesti et al., 2007; Rives, 2000).

About 100 mg of each sample was dehydrated at 400 °C in N_2 flow (40 cm^3/min) for 90 min and cooled to 120 °C, and then gaseous pyridine diluted in N_2 was allowed to pass through the samples for 60 min. The temperature was then kept at 120 °C under N_2 flow for 60 min to remove the physically adsorbed pyridine. After that, the samples were analyzed by TG/DTG and FTIR. The thermogravimetric analyses were performed under N_2 flow (40 cm^3/min) over the temperature range from 25 to 900 °C at a heating rate of 10 °C/min using a SHIMADZU thermobalance (TG/DTA) model DTG-60 H.

The number of acidic sites was calculated as follows: (i) from the total weight (w_{total}) of a sample with adsorbed pyridine (sample Py) analyzed by TG/DTG, the mass loss between 25 and 250 °C (w_{250}, usually water and/or physically adsorbed pyridine) was subtracted, thus obtaining the anhydrous weight sample; (ii) the amount of mass loss between 250 and 900 °C (w_{Py}, chemically adsorbed pyridine) was normalized for 1 g, dividing the obtained value by the anhydrous weight; (iii) the same calculation was accomplished using the curve TG/DTG of the sample without adsorbed pyridine; (iv) the weight of adsorbed pyridine was equal to the difference between normalized values for the sample with and without adsorbed pyridine; (v) using the pyridine molar weight (MWPy), the value for moles of adsorbed pyridine was then calculated. The mathematical representation of this procedure is in the equation below:

$$n_{Py} = \left\{ \underset{\text{Sample with Py}}{\left[w_{Py} / (w_{total} - w_{250}) \right]} - \underset{\text{Sample without Py}}{\left[w_{900} / (w_{total} - w_{250}) \right]} \right\} / MW_{Py}$$

where w_{900} = mass loss between 250 and 900 °C.

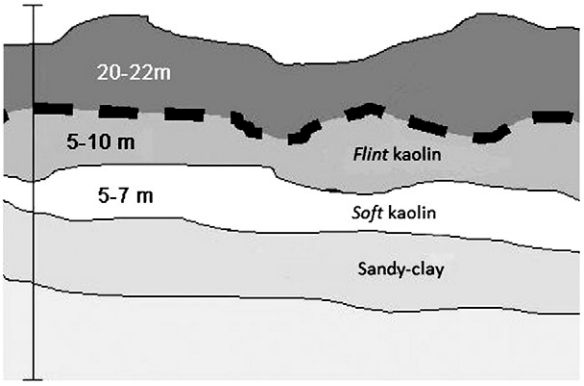

Fig. 1. Schematic geological profile of kaolin deposits [Carneiro et al., 2003].

Additionally, infrared spectra were recorded in the range 1700 to 1400 cm^{-1} by means of a Thermo IR100 spectrometer.

2.2.3. Catalytic tests

Prior to the experiments, the catalysts were activated at 130 °C in an oven for 90 min. The catalytic tests were performed using a PARR 4843 reactor. In a typical experiment, oleic acid was mixed with methanol and 5% of the solid acid catalyst (related to acid weight). The reaction mixture was kept under constant stirring (700 rpm) at 130 °C for 2 h. After completion of the reaction, the solid catalyst was separated by filtration. The percent of conversion of oleic acid into its ester was estimated by measuring the acid value of the product by titration with sodium hydroxide. The effects of time and temperature on the esterification of oleic acid using the leached metakaolins as catalysts were also investigated for this report.

3. Results and discussion

3.1. Characterization

3.1.1. Chemical compositions

The chemical compositions of the kaolins and leached metakaolins were determined by EDX, and the values are compared with those of theoretical kaolinite (Carneiro et al., 2003) in Table 1. From these characterizations, the materials were observed to have high TiO_2 content with the exception of the Century. This result could be explained by the presence of accessory minerals (as anatase) and/or the presence of isomorphically substituted Al (Carneiro et al., 2003). Furthermore, the leached metakaolins showed a Al_2O_3 content smaller than their parent kaolins. Century and *flint* were the most leached kaolin, which could be explained by the process used for the preparation of these kaolins. This process included the removal of sand and disaggregation steps that could have made the particles of Century and *flint* more accessible to acid attack than natural samples (KGa-1b and KGa-2) that must be passed through a grinding step.

3.1.2. XRD analysis

The XRD of all the kaolins studied (Fig. 2a) showed characteristic peaks for kaolinite at 2θ values of 12° and 24° (Carneiro et al., 2003). The main difference between the kaolins could be observed in the range of 20°<2θ>24°, which revealed the order degree of each kaolin. From the data, it is possible to affirm that KGa-1b and Century kaolins had a high degree of ordering while the KGa-2 and *flint* kaolins had a low degree of ordering.

In contrast, all of the leached metakaolins exhibited similar X-ray diffractograms (Fig. 2b). When the samples were calcined at 950 °C for 2 h, a water loss occurred and the kaolinite peaks disappeared, being replaced by a broad band between 20°<2θ>30° that could be attributed to an SiO_2 amorphous phase (Lenarda et al., 2007). The presence of three peaks at 2θ values of 30°, 44° and 56° were also

Table 1
Chemical compositions (wt.%) of kaolinite and the leached metakaolins.

Sample	SiO_2	Al_2O_3	TiO_2	Fe_2O_3	H_2O[a]
Theoretical kaolinite[b]	46.54	39.50	–	–	13.96
Flint kaolin	43.24	37.98	2.34	0.51	15.40
MF9S4	61.84	16.90	4.43	0.45	16.25
Century	45.60	39.0	0.65	0.53	14.1
MC9S4	85.03	7.37	1.85	0.15	5.60
KGa-1b[c]	43.36	38.58	1.67	0.35	15.05
M19S4	62.45	27.38	3.30	0.20	6.48
KGa-2[c]	43.49	38.14	1.91	1.15	15.03
M29S4	52.35	38.08	4.08	1.58	3.70

[a] Loss on ignition at 1000 ± 25 °C (wt.%).
[b] Carneiro et al., 2003.
[c] Mermut and Faz Cano, 2001.

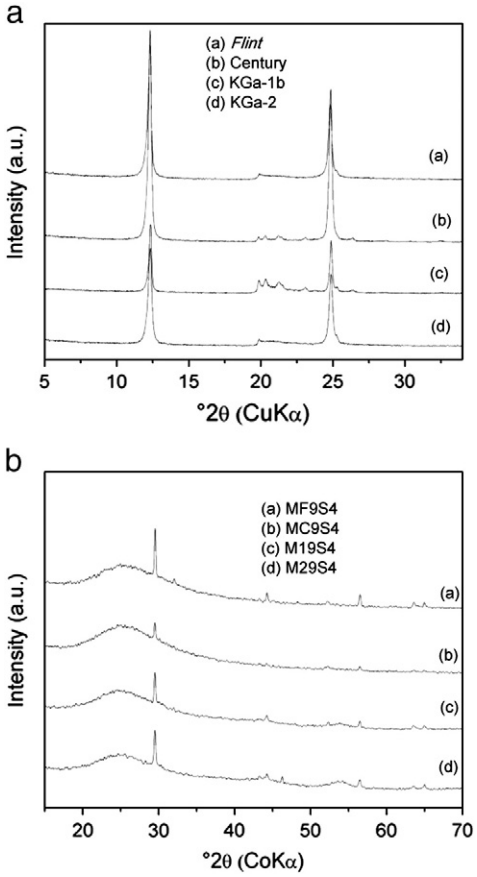

Fig. 2. X-ray diffractograms of the kaolins (a) and of the leached metakaolins (b).

observed that were related to anatase (TiO_2), a mineral frequently found in kaolin from the Capim region as well as in other kaolins (Carneiro et al., 2003). The XRD analysis also revealed that a complete breaking of the crystalline structure of the leached metakaolins occurred when compared to the parent kaolin. In addition, a structural water loss that facilitated the transformation of octahedral AlO_6 into tetra- and penta-coordinated Al units was also shown to occur (Massiot et al., 1995; Perissinotto et al., 1997). The literature reports that these Al units are more reactive and more susceptible to acid leaching, which is responsible for the partial dissolution of Al^{+3} and, consequently, the observed increase in the amorphous phase (Lenarda et al., 2007; Mermut and Faz Cano, 2001; Perissinotto et al., 1997; Sabu et al., 1999).

3.1.3. Scanning electron microscopy (SEM)

SEM micrographs of the kaolins showed that both *flint* (Fig. 3a) and KGa-2 (Fig. 3g) consisted of particles with sizes below 1 μm and were less well-defined than those observed in the Century (Fig. 3c) and KGa-1b (Fig. 3e) micrographs, which showed larger particles with a pseudo-hexagonal morphology. The SEM study also revealed that the leached metakaolins (Fig. 3b, d, f and h) were mainly formed by agglomerates of particles with rough surfaces (mainly MF9S4 and M29S4). SEM also showed a porosity related to spaces between these agglomerates, which were apparently larger for MC9S4 and M19S4. Larger particle size and the presence of agglomerates apparently led to less-dense material, as observed for Century and KGa-1b kaolins, which could explain their higher susceptibility to acid treatment when compared to the kaolins from the same region of origin.

3.1.4. N_2 adsorption–desorption

The observed N_2 adsorption–desorption isotherms (Fig. 4a and b) of type II based on the classification of IUPAC for acid-activated

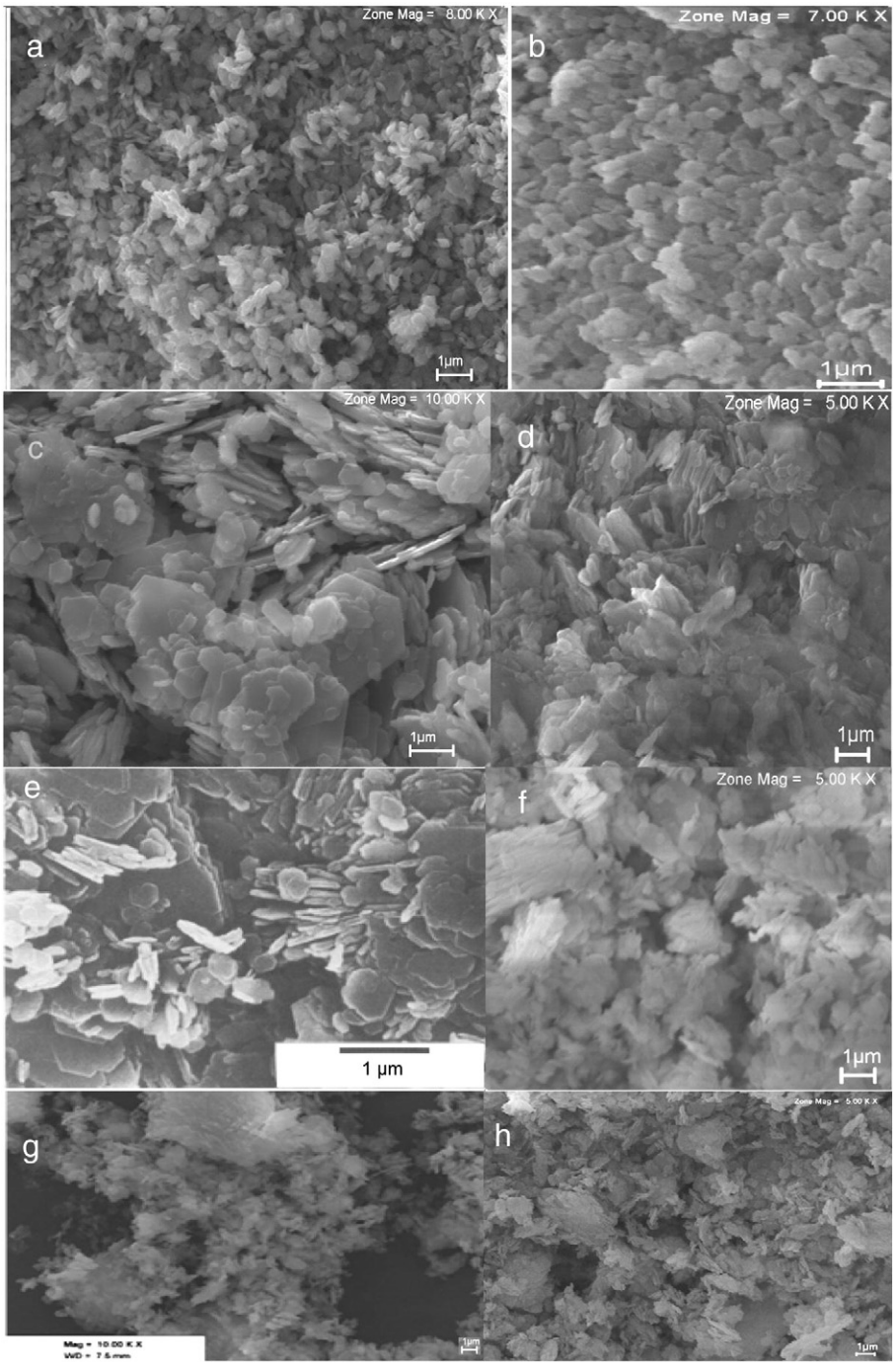

Fig. 3. SEM micrographs for a) *Flint* kaolin, b) MF9S4, c) Century, d) MC9S4, e) KGa-1b (Pruett and Webb, 1993), f) M19S4, g) KGa-2 (Pentrák et al., 2009) and h) M29S4.

metakaolins – with MF9S4 and M29S4 presenting a shape of type IIa, while MC9S4 and M19S4 present a shape of type IIb, according Rouquerol et al. (1999) – demonstrated that these materials possessed microporous structures and surface area values higher than their parental kaolins (Table 2). These characteristics resulted from acid leaching activity and, consequently, the amount of present amorphous silica in the sample became larger, with MF9S4 and MC9S4 presenting the largest increases in the values of surface area and microporous volume.

Considering that the microporous area and the microporous volume of the leached metakaolins also increased significantly, some of the acid-treated metakaolins could be considered interesting from a catalytic point of view, as materials with similar behavior were observed to have some catalytic activity (Perissinotto et al., 1997; Sabu et al., 1999). The specific surface area, microporous area and microporous volume values for the studied materials are listed in Table 2.

3.1.5. Acidity of activated metakaolins

The literature showed that pyridine was a suitable probe to measure the surface acidity of porous materials and was able to provide quantitative analysis of the acidic sites by TPD (Ghesti et al., 2007; Parrillo et al., 1990). Furthermore, FTIR of adsorbed pyridine has become routine in catalysis laboratories and can differentiate Brønsted, Lewis and hydrogen-bonded sites (Ghesti et al., 2007; Parry, 1963). Based on this information, the acidity studies in this work were performed using the methodology described by Ghesti et al. (2007), which uses TG/DTG and FTIR after pyridine adsorption.

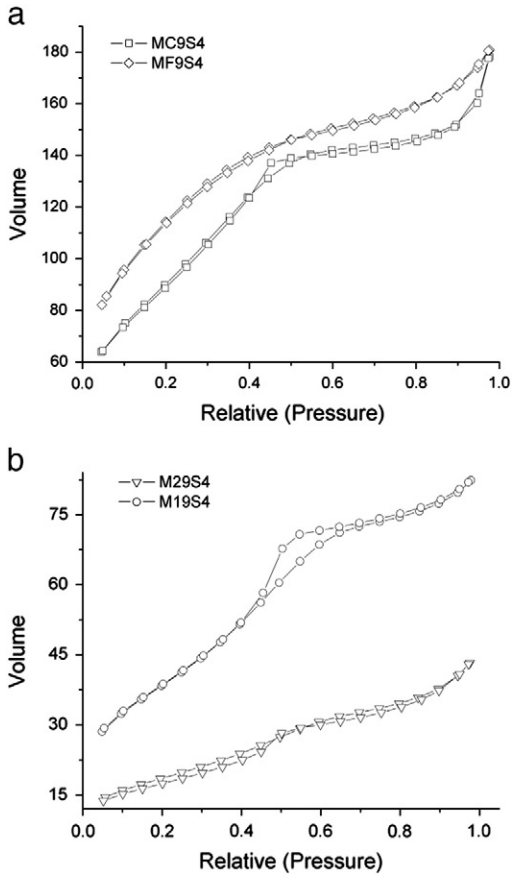

Fig. 4. N_2 adsorption–desorption isotherms of the acid-activated metakaolins: a) MF9S4 and MC9S4, b) M19S4 and M29S4.

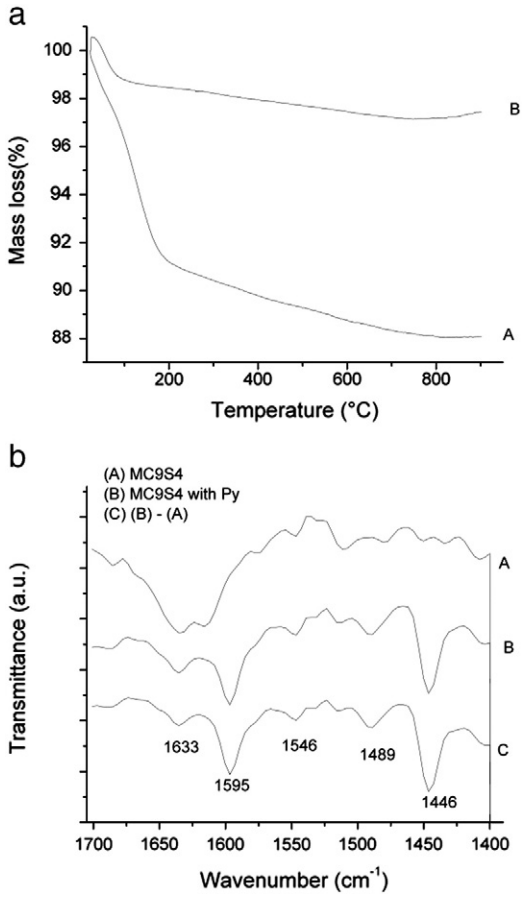

Fig. 5. a) TG curves of MC9S4 with (A) and without adsorbed pyridine (B). b) IR spectra in the region 1700–1400 cm^{-1} for MC9S4 with adsorbed pyridine.

This method proved to be a good alternative to TPD profiles for the characterization of heterogeneous catalysts (Ghesti et al., 2007). The TG curves for all the leached metakaolins (illustrated for MC9S4 in Fig. 5a) showed a behavior similar to that described by Belver et al. (2002). This behavior described two different processes: a rapid mass loss at temperatures between 25 and 100 °C associated with adsorbed water, and a continuous second loss between 250 and 900 °C attributed to dehydroxylation from either $Si(OSi)_3OH$ groups formed during preparation or water molecules fixed at specific sites of the solids. Both of these groups were again probably coordinated to the remaining Al cations.

TG curves of the samples with adsorbed pyridine presented higher mass loss compared to those samples without adsorbed pyridine, probably due to a loss between 150 and 250 °C assigned to physically adsorbed water and pyridine as well as a continuous loss above 250 °C attributed to the loss of chemically adsorbed pyridine. Among the analyzed samples, MC9S4 showed the highest difference in mass loss between the sample with pyridine and the sample without pyridine. Therefore, the methodology described by Ghesti et al. (2007) using TG/DTG and FTIR after pyridine adsorption was used to define the acidity of the leached metakaolins.

Analyzing Table 2, it was observed that the acidity of each material resulted directly from the Al content of that sample. As such, the samples with less Al content showed a higher density of acidic sites, which could be attributed to the scattering of Al cations during acid leaching, making them more accessible and reactive. These results were in agreement with those obtained by Sabu et al. (1999), who reported that acid treatment of metakaolins resulted in the relocation of Al cations from the internal structure to the newly created pores; those cations then acted as Brönsted acid centers in the presence of water molecules and as Lewis acid centers under anhydrous conditions.

The infrared spectra of the samples with adsorbed pyridine in the region 1700 to 1400 cm^{-1} (Fig. 5b) showed typical bands that could be assigned to Lewis site-bonded pyridine near at 1446 and Brönsted site-bonded pyridine at 1546 and 1633 cm^{-1}. In addition, there was a band at approximately 1489 cm^{-1} that could be attributed to pyridine molecules associated with both Brönsted and Lewis acidic sites, and a band at 1595 cm^{-1} was related to weak hydrogen bonding to surface pyridine molecules. This profile agreed with that presented by other leached metakaolins (Perissinotto et al., 1997), confirming the nature of the acidic sites on acid-activated metakaolins.

Table 2
Specific surface area, microporous area, microporous volume values of the kaolins and the leached metakaolins and the number of acidic sites on the leached metakaolins.

Sample	S.A.[a] (m^2/g)	Aμ[b] (m^b/g)	Vμ[c] (cm^c/g)	Number of acid sites (μmolPy/g)
Flint	24	11	0.006	
MF9S4	406	319	0.15	237.7
Century	9	4	0.006	
MC9S4	335	233	0.115	250.5
KGa-1b	12	6	0.008	
M19S4	138	80	0.05	163.4
KGa-2	20	10	0.01	
M29S4	65	34	0.02	21.9

[a] Specific surface area calculated by BET.
[b] Aμ = Microporous area calculated by *t*-plot.
[c] Vμ = Microporous volume calculated by *t*-plot.

Table 3
Esterification at 130 °C between oleic acid and methanol (1:60) after 120 min.

Catalyst	Conversion (wt%)
–	13.8
MF9S4	62.5
MC9S4	86.4
M19S4	53.0
M29S4	24.9

3.2. Catalytic tests

The catalytic activity of the acid-activated metakaolins for the esterification of oleic acid was determined from the acidity index of the final product. Table 3 shows the effect of each catalyst on the esterification reaction with methanol. The analysis of the obtained results showed that final conversion was directly related to the level of Al in the sample resulting from acid leaching. When a larger distribution of Al on the surface of the leached metakaolin was available, it facilitated access of the reactants to the acidic sites, resulting in a larger conversion value.

3.2.1. Influence of temperature

The normal behavior for the catalyzed reactions was an increase in conversion rate when the temperature was increased (Ghesti et al., 2009; Gokulakrishnan et al., 2007). Using an acid:alcohol molar ratio of 1:60, the esterification of oleic acid with methanol was performed at 100, 115, 130 and 160 °C, and the results (Fig. 6) were consistent with this behavior. In fact, it was possible to confirm that the temperature was crucial to increase the conversion in the presence of the catalysts, especially for MF9S4, which increased from 8.1% at 100 °C to a 95.3% conversion at 160 °C.

3.2.2. Influence of reaction time

The effect of reaction time was studied using the 1:60 (acid: alcohol) molar ratio at 100, 115, 130 and 160 °C. Analyzing the results shown in Table 4, it could be observed that the reaction occurred more rapidly up to 2 h, after which the conversion increased to a lesser extent. The gradual increase of the conversion when the reaction time was increased is a natural characteristic of reactions such as this one (Gokulakrishnan et al., 2007).

After 2 h of reaction (except for M29S4), the yields reach a near saturation of conversion. This behavior is similar to that described by Oliveira et al. (2010) using modified heteropoliacid, which affirm that as the yielded water increases in an esterification process, the reaction kinetics decrease possibly due to competition between the substrate and water for sorption on the active sites of the catalyst, and the increase of the reverse hydrolysis rate.

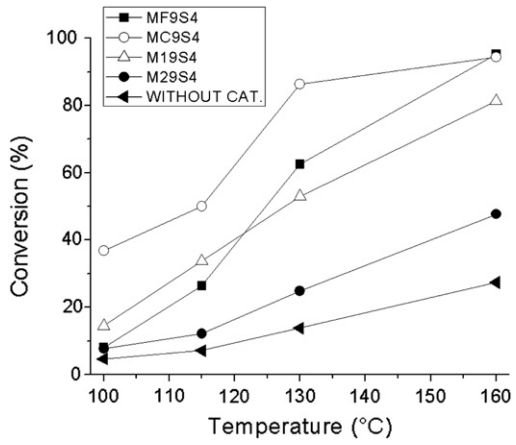

Fig. 6. Effect of temperature on conversion. Acid:alcohol ratio of 1:60 and 120-min reaction time.

Table 4
Effect of time on esterification rate of oleic acid with methanol (1:60).

T (°C)	Catalyst	30 min	60 min	120 min	240 min
100	–	1.3	2.5	4.7	8.2
115	–	2.2	3.9	7.1	11.4
130	–	4.2	8.1	13.8	22.0
160	–	6.7	12.1	27.4	42.0
100	MF9S4	2.6	4.4	8.1	13.5
115	MF9S4	8.5	17.1	26.4	44.0
130	MF9S4	28.9	44.1	62.5	84.2
160	MF9S4	55.0	79.0	95.3	98.9
100	MC9S4	11.8	21.5	36.8	59.4
115	MC9S4	17.0	32.2	50.0	74.4
130	MC9S4	39.8	64.0	86.4	96.8
160	MC9S4	62.6	77.6	94.4	98.8
100	M19S4	5.5	10.1	14.5	23.1
115	M19S4	8.6	18.0	33.7	45.3
130	M19S4	18.8	32.0	53.0	68.0
160	M19S4	40.9	52.7	81.4	94.8
100	M29S4	2.7	3.9	7.7	12.9
115	M29S4	5.1	8.4	12.2	19.8
130	M29S4	7.8	12.3	24.9	38.0
160	M29S4	17.4	27.2	47.7	72.0

Several papers have described first-order kinetics for esterification reactions (Carmo Jr. et al., 2009; Gokulakrishnan et al., 2007; Kirumakki et al., 2006; Palani and Pandurangan, 2005). In this work, determining the order of the esterification reaction of oleic acid with methanol was accomplished using the classical definitions of chemical kinetics and considering oleic acid as the limiting reagent, whose transformation into esters follows the acidity index. In order to determine the order of the reaction by an elementary kinetic theory, a complete conversion of the acid was assumed. A linear relation was found between all experimental data when (-ln (1-conversion)) was plotted as a function of reaction time (figures not shown). The resulting regression coefficients of the straight lines showed good fits to first-order kinetics.

Table 5 presents some esterification results found in the literature compared with some results obtained in this work. By analyzing this table, it was possible to confirm that the results obtained using MF9S4 as a catalyst for esterification of oleic acid with methanol were quite satisfactory because they were similar or higher than other catalysts presented in the literature (Carmo Jr. et al., 2009; Gokulakrishnan et al., 2007; Palani and Pandurangan, 2005; Rabindran Jermy and Pandurangan, 2005). Additionally, these other catalysts had

Table 5
Esterification reaction conversions with different catalysts.

Acid	Alcohol	Alcohol/acid	Temp. (°C)	Catalyst	Conversion (%)	Ref
Acetic	1-Butyl	½	125	Al-MCM-41 (Si/Al = 25)	87.3	[a]
Acetic	1-Propyl	½	150	Al-MCM-41 (Si/Al = 30)	83.7	[b]
Acetic	Amilic	½	250	Al-MCM-41 (Si/Al = 100)	91.0	[c]
Palmitic	Methyl	60/1	130	Al-MCM-41 (Si/Al = 8)	79.0	[d]
Palmitic	Ethyl	60/1	130	Al-MCM-41 (Si/Al = 8)	67.0	[d]
Oleic	Methyl	60/1	130	MC9S4	96.8	[e]
Oleic	Methyl	60/1	160	MF9S4	98.9	[e]
Oleic	Methyl	60/1	160	M19S4	94.8	[e]

[a] Rabindran Jermy and Pandurangan, 2005 (reaction time — R.T.: 480 min).
[b] Gokulakrishnan et al., 2007 (R.T.: 480 min).
[c] Palani and Pandurangan, 2005 (R.T.: 60 min).
[d] Carmo Jr. et al., 2009 (R.T.: 120 min).
[e] Present work (R.T.: 240 min).

production costs much higher than acid-activated metakaolins prepared from low-cost raw materials.

4. Conclusions

We observed that the removal of sand and disaggregation may have made the Century and *flint* kaolins more susceptible to acid leaching than KGa-1b and KGa-2. When kaolins from the same region were compared, it was possible to observe that the well-ordered kaolins were more effectively leached a finding that could be related to the presence of larger particles that led to the formation of agglomerates that were less dense and more accessible to acid attack.

Some activated metakaolins presented a considerable increase in surface area in addition to a high microporous volume. The acidity evaluation of the acid-activated metakaolins confirmed the presence of both Brönsted and Lewis acid sites, with MC9S4 presenting the highest values.

All of the leached metakaolins studied showed catalytic activity for the esterification of oleic acid with methanol. The analysis of conversion values obtained revealed a correlation with Al content and acidity for each prepared sample. In fact, MC9S4 was the sample with the lowest Al content and the greatest number of acid sites and, therefore, the highest conversion values.

These results indicated that kaolin could be considered a promising raw material for the production of catalysts for the esterification of oleic acid with methanol. It is important to emphasize that one of the kaolins (the Amazon *flint* kaolin) was previously regarded as a reject, which makes its utilization for the production of sustainable fuels all the more interesting.

Acknowledgments

The authors thank CNPq, FINEP, SEDUC/CAPES, PRONEX/FAPESPA and LAPAC/UFPA for financial support.

References

Araújo Melo, D.M., Ruiz, J.A.C., Melo, M.A.F., Sobrinho, E.V., Schmall, M., 2000. Preparation and characterization of terbium palygorskite clay as acid catalyst. Microporous Mesoporous Mater. 38, 345–349.

Belver, C., Muñoz, M.A.B., Vicente, M.A., 2002. Chemical activation of a kaolinite under acid and alkaline conditions. Chem. Mater. 14, 2033–2043.

Boz, N., Degirmenbasi, N., Kalyon, D.M., 2009. Conversion of biomass to fuel: transesterification of vegetable oil to biodiesel using KF loaded nano-γ-Al_2O_3 as catalyst. Appl. Catal. B 89, 590–596.

Carmo Jr., A.C., de Souza, L.K.C., Costa, C.E.F., Longo, E., Zamian, J.R., Rocha Filho, G.N., 2009. Production of biodiesel by esterification of palmitic acid over mesoporous aluminosilicate Al-MCM-41. Fuel 88, 461–468.

Carneiro, B.S., Angélica, R.S., Scheller, T., de Castro, E.A.S., Neves, R.F., 2003. Mineralogical and geochemical characterization of the hard kaolin from the Capim region, Pará, northern Brazil. Cerâmica 49, 237–244.

Centi, G., Perathoner, S., 2008. Catalysis by layered materials: a review. Microporous Mesoporous Mater. 107, 3–15.

Flessner, U., Jones, D.J., Rozière, J., Zajac, J., Storaro, L., Pavan, M., Jiménez-López, A., Rodríguez-Castellón, E., Trombetta, M., Busca, G., 2001. A study of the surface acidity of acid-treated montmorillonite clay catalysts. J. Mol. Catal. A Chem. 168, 247–256.

Ghesti, G.F., de Macedo, J.L., Parente, V.C.I., Dias, J.A., Dias, S.C.L., 2007. Investigation of pyridine sorption in USY and Ce/USY zeolites by liquid phase microcalorimetry and thermogravimetry studies. Microporous Mesoporous Mater. 100, 27–34.

Ghesti, G.F., de Macedo, J.L., Parente, V.C.I., Dias, J.A., Dias, S.C.L., 2009. Synthesis, characterization and reactivity of Lewis acid/surfactant cerium trisdodecylsulfate catalyst for transesterification and esterification reactions. Appl. Catal. A 355, 139–147.

Gokulakrishnan, N., Pandurangan, A., Sinha, P.K., 2007. Esterification of acetic acid with propanol isomers under autogeneous pressure: a catalytic activity study of Al-MCM-41 molecular sieves. J. Mol. Catal. A Chem. 263, 55–61.

Jacobson, K., Gopinath, R., Meher, L.C., Dalai, A.K., 2008. Solid acid catalyzed biodiesel production from waste cooking oil. Appl. Catal. B 85, 86–91.

Kantam, M.L., Bhaskar, V., Choudary, B.M., 2002. Direct condensation of carboxylic acids with alcohols: the atom economic protocol catalysed by Fe^{3+}-Montmorillonite. Catal. Lett. 78, 185–188.

Kirumakki, S.R., Nagaraju, N., Chary, K.V.R., 2006. Esterification of alcohols with acetic acid over zeolites Hβ, HY and HZSM5. Appl. Catal. A 299, 185–192.

Kotschoubey, B., Truckenbrodt, W., Hieronymus, B., 1996. Depósitos de caulim e argila semi-flint no nordeste do Estado do Pará. Rev. Bras. Geocienc. 26 (2), 71–80.

Lenarda, M., Storaro, L., Talon, A., Moretti, E., Riello, P., 2007. Solid acid catalysts from clays: preparation of mesoporous catalysts by chemical activation of metakaolin under acid conditions. J. Colloid Interface Sci. 311, 537–543.

Liu, R., Wang, X., Zhao, X., Feng, P., 2008. Sulfonated ordered mesoporous carbon for catalytic preparation of biodiesel. Carbon 46, 1664–1669.

López, D.E., Goodwin Jr., J.G., Bruce, D.A., Furuta, S., 2008. Esterification and transesterification using modified-zirconia catalysts. Appl. Catal. A 339, 76–83.

Marchetti, J.M., Errazu, A.F., 2008. Esterification of free fatty acids using sulfuric acid as catalyst in the presence of triglycerides. Biomass Bioenergy 32, 892–895.

Massiot, D., Dion, P., Alcover, J.F., Bergaya, F., 1995. ^{27}Al and ^{29}Si MAS NMR study of kaolinite thermal decomposition by controlled rate thermal analysis. J. Am. Ceram. Soc. 78 (11), 2940–2944.

Mbaraka, I.K., Shanks, B.H., 2006. Acid strength variation due to spatial location of organosulfonic acid groups on mesoporous silica. J. Catal. 244, 78–85.

Mbaraka, I.K., Radu, D.R., Lin, V.S.-Y., Shanks, B.H., 2003. Organosulfonic acid-functionalized mesoporous sílicas for the esterification of fatty acid. J. Catal. 219, 329–336.

Mermut, A.R., Faz Cano, A., 2001. Baseline studies of the Clay Minerals Society source clays: chemical analyses of major elements. Clays Clay Miner. 49 (5), 381–386.

Mo, X., Lotero, E., Lu, C., Liu, Y., Goodwin, J.G., 2008. A novel sulfonated carbon composite solid acid catalyst for biodiesel synthesis. Catal. Lett. 123, 1–6.

Oliveira, C.F., Dezaneti, L.M., Garcia, F.A.C., de Macedo, J.L., Dias, J.A., Dias, S.C.L., Alvim, K.S.P., 2010. Esterification of oleic acid with ethanol by 12-tungstophosphoric acid supported on zirconia. Appl. Catal. A 372, 153–161.

Palani, A., Pandurangan, A., 2005. Esterification of acetic acid over mesoporous Al-MCM-41 molecular sieves. J. Mol. Catal. A Chem. 226, 129–134.

Parrillo, D.J., Adamo, A.T., Kokotailo, G.T., Gorte, R.J., 1990. Amine adsorption in H-ZSM-5. Appl. Catal. 67, 107–118.

Parry, E.P., 1963. An infrared study of pyridine adsorbed on acidic solids. Characterization of surface acidity. J. Catal. 2, 371–379.

Pentrák, M., Madejová, J., Komadel, P., 2009. Acid and alkali treatment of kaolins. Clay Miner. 44, 511–523.

Perissinotto, M., Lenarda, M., Storaro, L., Ganzerla, R., 1997. Solid acid catalysts from clays: acid leached metakaolin as isopropanol dehydration and 1-butene isomerization catalyst. J. Mol. Catal. A Chem. 121, 103–109.

Pruett, R.J., Webb, H.L., 1993. Sampling and analysis of Kga-1B well-crystallized kaolin source clay. Clays Clay Miner. 41 (4), 514–519.

Rabindran Jermy, B., Pandurangan, A., 2005. Catalytic application of Al-MCM-41 in the esterification of acetic acid with various alcohols. Appl. Catal. A 288, 25–33.

Rezende, M.J.C., 2006. Uso de Argila Brasileira como Catalisador na Produção de Biodiesel. Ph.D. Thesis, UFRJ, Rio de Janeiro, Brazil. Unpublished results.

Rives, V., 2000. Characterisation by thermal techniques. Catal. Today 56, 357–359.

Rouquerol, J., Rouquerol, F., Sing, K., 1999. Adsorption by Powders and Porous Solids: Principles, Methodology and Applications, first ed. Academic Press, London.

Sabu, K.R., Sukumar, R., Rekha, R., Lalithambika, M., 1999. A comparative study on H_2SO_4, HNO_3 and $HClO_4$ treated metakaolinite of a natural kaolinite as Friedel-Crafts alkylation catalyst. Catal. Today 49, 321–326.

Srilatha, K., Lingaiah, N., Prabhavathi Devi, B.L.A., Prasad, R.B.N., Venkateswar, S., Sai Prasad, P.S., 2009. Esterification of free fatty acids for biodiesel production over heteropoly tungstate supported on niobia catalysts. Appl. Catal. A 365, 28–33.

Vaccari, A., 1999. Clays and catalysis: a promising future. Appl. Clay Sci. 14, 161–198.

Xu, L., Li, W., Hu, J., Yang, X., Guo, Y., 2009. Biodiesel production from soybean oil catalyzed by multifunctionalized Ta_2O_5/SiO_2-[$H_3PW_{12}O_{40}$/R] (R = Me or Ph) hybrid catalyst. Appl. Catal. B 90 (3–4), 587–594.

Zheng, S., Kates, M., Dubé, M.A., McLean, D.D., 2006. Acid–catalyzed production of biodiesel from waste frying oil. Biomass Bioenergy 30, 267–272.